RESEARCH



Comparative analyses of immune gene profiles and antioxidant capabilities in the midgut and liver of three species of grass carps (Ctenopharyngodon idella) following gut infection with Aeromonas hydrophila

Wei-Sheng Luo¹ · Zi-Han Xu¹ · Qin-Yang He¹ · Jie Peng¹ · Fei Wang¹ · Jian Li¹ · Sheng-Wei Luo¹

Received: 24 June 2024 / Accepted: 24 July 2024 / Published online: 30 July 2024 © The Author(s), under exclusive licence to Springer Nature Switzerland AG 2024

Abstract

Aeromonas hydrophila is an important etiologic agent, triggering an increased trend of disease outbreak in fish farming. In this investigation, we evaluated pathological response in the midgut and liver of three types of grass carps after gut infection. Severe pathological levels of tissue necrosis were observed in common grass carp (GC) and gynogenetic grass carp (GGC), but mild pathological symptom was detected in hybrid grass carp (DRGC), along with the dramatically increased number of goblet cells. Moreover, three types of grass carps showed upregulated levels of immune gene patterns and antioxidant abilities, whereas inflammatory cytokine expression levels in hybrid grass carp (DRGC) were lower than that of gynogenetic grass carp (GGC) and common grass carp (GC). These results suggested that DRGC may exhibit a disease tolerance against *A. hydrophila*-induced tissue inflammation.

Keywords Grass carp · Gene expressions · Antioxidant ability · Gut tract

Introduction

Among cultivated fish species, grass carp occupies a dominant position in Chinese aquaculture, but it frequently suffers from various infectious diseases, which may show a detrimental impact on its farming process (Xie et al. 2018). Although large numbers of immune-associated properties are found in teleost fish (Magnadottir 2010), such as cytokine production and secretion (Secombes et al. 2001), complement cascades (Kania

Handling Editor: Brian Austin

Wei-Sheng Luo and Zi-Han Xu contributed equally to this work.

State Key Laboratory of Developmental Biology of Freshwater Fish, Engineering Research Center of Polyploidy Fish Reproduction and Breeding of the State Education Ministry, College of Life Science, Hunan Normal University, Changsha 410081, People's Republic of China



Sheng-Wei Luo swluo1@163.com; swluo@hunnu.edu.cn

and Buchmann 2022), and pathogen-recognizing clusters (Boltaña et al. 2011), pollutants and ambient stressors can rapidly suppress immune function and disorder physiological disorder, which can render fish more susceptible to invading pathogens (Reid et al. 1997). In addition, antibiotic accumulation may markedly challenge microbial community to increase the proportion of resistant pathogens, which may lead to increasing trend of microbial infection in aquaculture (Yuan et al. 2023).

When referring to fish breeding, hybridization may generally enable hybrid offsprings to develop novel abilities, including disease resistance and rapid growth performance, through alteration of gene structures and expressions (Bullini 1985). Our previous studies indicated that hybrid cyprinid fish showed a higher disease tolerance than its parents (Xiong et al. 2022, 2021). In addition, hybrid cyprinid fish possessed increased activities of digestive enzymes and gut flora by comparing with its parental species, which may be associated with its faster growth rate (Wang et al. 2023a). Currently, researchers have paid increasing attention to the study on the synergistic regulation of the gut tract and liver in teleosts (Wu et al. 2016). In general, the reciprocal connection of the liver, gut tract, and gut flora may play the predominant role in immune surveillance against invading pathogens (Zeuzem 2000). For instance, gut flora can restrict pathogenic colonization, regulate immunoglobulin production as well as facilitate lymphocyte recruitment, while metabolites from the gut tract may significantly influence innate immunity in the liver upon infection (Trivedi and Adams 2016). Nevertheless, recent findings indicate that some invasive pathogens can effectively escape the host immune surveillance and then elevate disease-induced inflammatory response at infection loci after the breach of mucosal barrier (Pickard et al. 2017). Afterwards, pathogenic bacteria may further invade extragut organs for deep infection, while the liver may subsequently receive bacterial products and metabolites from the gut tract for detoxification (Giuffrè et al. 2020). Among reported issues, A. hydrophila is one of the serious pathogens in aquatic environment, which can enhance the morbidity of farmed fish by producing different types of bacterial toxins (Howard et al. 1987). Our preliminary investigation demonstrated that increased levels of tissue injury and antioxidant collapses were found in A. hydrophila-infected cyprinid fish (Wang et al. 2023b). In addition, inflammatory cytokine could dysregulate mucosal immunity and then aggravate A. hydrophila-induced injury in gut-liver axis of crucian carp (Xiong et al. 2023; Li et al. 2024). Although previous findings have claimed the advantage in survival and growth rates of DRGC (Wang et al. 2022), there are few studies on regulation in immune signals in the midgut and liver of hybrid grass carps and its parental species.

Therefore, we aimed to assess pathological features, gene profiles, and redox enzymatic activities in the midgut and liver of three types of juvenile grass carps after gut infection. This research may offer a newly finding into immune feature of hybrid fish.

Materials and methods

Ethical statement

All procedures, including the care and use of experimental fish, were approved by the Animal Care and Use Committee of Hunan Normal University (Changsha City, Hunan province, China) and the Technical Committee for Laboratory Animal Sciences of the Standardisation Administration of China (SAC/TC281), and performed under the national standard Guidelines for Ethical Review of Animal Welfare (GB/T 35892–2018).



Fish preparation

Healthy juvenile GC, GGC, and DRGC (average length 16.28 ± 0.87 cm) were collected from a farming base (Wangcheng district, Changsha, China). Fish were daily fed with commercial diets (2 mm, Tongwei Co., Ltd., China) for 2-week acclimation in clean circulating water (21–24 °C, pH 7.6–8.2) till 24 h before infection experiment. Fish feed and feces were removed daily to avoid pathogenic contamination during fish acclimation and infection periods. Before the infection experiment, liver tissues were randomly isolated from GC, GGC, and DRGC to confirm healthy status. No amplification of *A. hydrophila hlyA* gene was detected by using DNA templates of isolated livers (Fig. S1).

Infection by bacterial perfusion

PBS suspension of *A. hydrophila* L3-3 (OM184261, 1×10^8 CFU mL⁻¹) was used for perfusion assay based on our previous study (Wang et al. 2023c). Thirty fish of each species were randomly divided and sacrificed for mortality statistics, tissue section, bacterial load, biochemistry analysis, and gene expression. In brief, fish were gut perfused with *A. hydrophila* L3-3 by using a gavage needle inserted into a depth of approximately 3 cm, whereas equivalent volume of sterile PBS perfusion was used as control group. The liver, midgut, trunk kidney, and spleen were collected at 72-h post-infection. Afterwards, isolated tissues were immediately frozen in liquid nitrogen and stored in -80 °C.

Pathological section assay

After tissue fixation by Bouin's solution, paraffin-embedded midgut and liver were performed as previously described (Ma et al. 2021). In brief, Bouin-fixed tissues were dehydrated in gradient alcohol (70% ethanol, overnight; 80%, 90%, 95%, and 100% ethanol, 15 min each; xylene+100% ethanol (1:1) and xylene, 30 min each), followed by paraffin infiltration and embedment. According to the manufacturer's instructions, midgut slices, and liver slices were stained by using a periodic acid-schiff (PAS) kit (Beyotime Biotechnology, China) and hematoxylin and eosin (HE) staining kit (Beyotime Biotechnology, China), respectively. Then, pathological sections were observed by using a light microscope (Leica DM 4000 with Leica Q Vin 3 program). The experiment possessed three biological repeats (n=3).

DNA isolation for bacterial load assay

Genomic DNA was extracted from the liver, midgut, trunk kidney, and spleen of GC, GGC, and DRGC by using a tissue DNA extraction kit (Magen Biotechnology, China). Before use, DNA concentration was adjusted to 100 ng/µL before use.

RNA extraction, cDNA synthesis, and gene expression analysis

Total RNA was isolated from the midgut and liver and treated with DNAase to avoid genomic DNA contamination by using FastPure cell/tissue total RNA isolation Kit v2



(Vazyme Biotech, China). After RNA quality check, 1000 ng of purified total RNA was used for cDNA synthesis by using MonScript™ RT III All-in-One Mix with dsNase (Monad, China) (Li et al. 2024).

Relative levels of *A. hydrophila* L3-3 *hlyA* gene and immune-related genes were measured by quantitative real-time PCR (qRT-PCR) assay. For bacterial load assay, relative expressions of *A. hydrophila hlyA* gene were detected in the liver, trunk kidney, spleen, and intestine, while *gapdh* was used as reference gene. For immune-related gene detection, relative expressions of *cytokines* (*cl12a*, *cxcl14*, *cxcl18b*, *il1β*, *il6*, *il8*, *il19*, *il34*, *ccl2*, *ccl8*, *ccl20*, *tnfα*), *mucins* (*Muc2*, *Muc4*, *Muc5e*, *Muc13a*, *Muc15*, *Muc21*), *immunoglobulins* (*IgM*, *IgT/Z*), *cluster of differentiation antigen* (*cd4*, *cd8α*), *myeloperoxidase* (*mpo*), *NK-lysin* and *hepcidin* were investigated. *18 s rRNA* was used as reference gene. In addition, qRT-PCR reaction contained: 10.0 µL SYBR Green Master Mix (ABI), 2.0 µL DNA/cDNA template, 0.5 µL each primer, and 7.0 µL ddH₂O. The program contained 1 cycle of 95 °C for 30 s, 40 cycles of 95 °C for 15 s, 60 °C for 35 s, followed by 1 cycle of 95 °C for 30 s, 60 °C for 60 s. At the end of qRT-PCR amplified reactions, the melting curve analysis was implemented to confirm the credibility of each qRT-PCR analysis. Results were calculated by 2 $^{-\Delta\Delta Ct}$ method. The primers are presented in Table. S1. The experiment possessed three biological repeats (*n* = 3).

Evaluation of antioxidant ability

The isolated midgut and liver were homogenized in ice-cold 1×PBS buffer. Following centrifugation at 10,000×g for 10 min at 4 °C, the supernatants were quantified by using bicinchoninic acid (BCA) method.

Catalase (CAT) activities in the midgut and liver were detected at OD_{405} absorbance by using a CAT activity kit (Nanjing Jiancheng Bioengineering Institute, China). Results were presented as units of CAT activity per milligram of protein, where 1 U of CAT is defined as the amount of enzyme decomposing 1 μ mol H_2O_2 per second. The experiment possessed three biological repeats (n=3).

Succinate dehydrogenase (**SDH**) activities in the midgut and liver were detected at OD_{600} absorbance by using a **SDH** activity kit (Nanjing Jiancheng Bioengineering institute, China). Mean values were shown as U **SDH** per milligram of protein. The experiment possessed three biological repeats (n=3).

Glutathione peroxidase (**GPx**) activities in the midgut and liver were observed at OD_{340} absorbance by using a **GPx** activity kit (Beyotime Biotechnology, China). Results were shown as U **GPx** activity per gram of protein. The experiment possessed three biological repeats (n=3).

Lactate dehydrogenase (**LDH**) activities in the midgut and liver were observed at OD_{490} nm by using a **LDH** kit (Beyotime Biotechnology, China). Results were shown as U **LDH** activity per milligram of protein. The experiment possessed three biological repeats (n=3).

Glutathione reductase (**GR**) activities in the midgut and liver were observed at OD_{412} nm by using a **GR** kit (Nanjing Jiancheng Bioengineering Institute, Nanjing, China). Results were shown as U **GR** activity per gram of protein. The experiment possessed three biological repeats (n=3).

Monoamine oxidase (MAO) activities in the midgut and liver were detected at OD_{242} nm by using a MAO kit (Nanjing Jiancheng Bioengineering Institute, China). Results were shown as U MAO activity per milligram of protein. The experiment possessed three biological repeats (n=3).



Statistical analyses

The qRT-PCR results and enzymatic activities in tissues were subjected to T-test analysis by using SPSS 17.0 software. If the analytical levels reach less-than 0.05 *p*-value, results were statistically significant with different letters. In addition, results of qRT-PCR and enzymatic data were calculated by principal component analysis (PCA).

Results

Bacterial loads in tissues

Survival rates of DRGC were higher than that of GC and GGC after gut infection with A. hydrophila L3-3 during monitor periods (Fig. S2). In order to compare the infectious status in three species of grass carps, bacterial load assay was performed at 72-h post-infection. GC receiving bacterial infection showed 1.6-, 3.2-, 1.5-, and 2.1-fold increase of hlyA gene expression in the liver, midgut, trunk kidney, and spleen (p < 0.05) (Fig. 1A). In Fig. 1B, 1.6-, 1.6-, 2.8-, and 2.5-fold increase of hlyA gene expression was detected in the liver, midgut, trunk kidney, and spleen of GGC at 72 h (p < 0.05). In addition, relative expression of hlyA gene in the liver, midgut, trunk kidney, and spleen of DRGC increased by 1.5-, 1.8-, 1.4-, and 2.7-fold at 72 h upon infection (p < 0.05).

Pathological observation

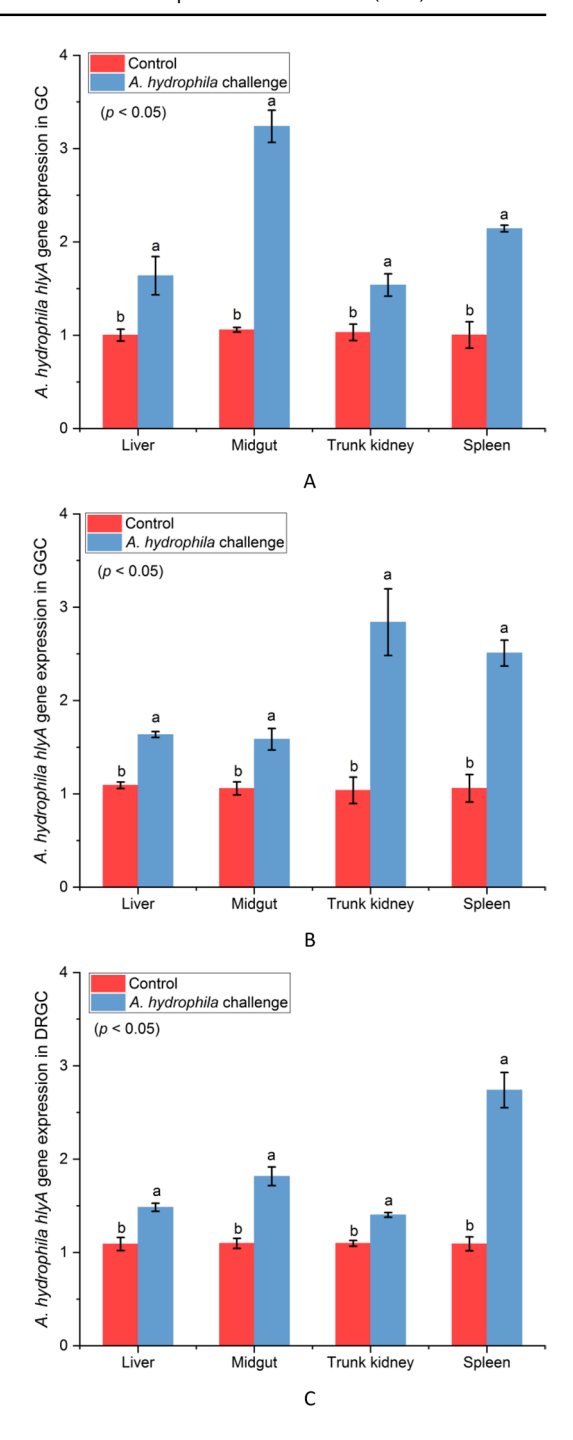
To compare injury levels of the midgut and liver, tissue section assay was carried out. In Fig. 2A–C, gut infection with strain L3-3 could dramatically induce different degree of tissue injury in the midgut and liver of GC, GGC, and DRGC. Severe tissue necrosis, villous deformation, and villous vacuolization occurred in the midgut of GC and GGC at 72-h post-infection, while mild pathological symptom was observed in the midgut of DRGC. A significant decrease of villous aspect ratios in the midgut was detected in GC, GGC, and DRGC upon infection. In contrast, goblet cell numbers decreased dramatically in GC and GGC after strain L3-3 infection, while goblet cell numbers in DRGC increased sharply (p<0.05). Moreover, liver pathological levels of tissue necrosis, vacuolation, and nuclear displacement appeared to be more severe than that of DRGC (Fig. 3). These results suggested that the differences of pathological symptoms were observed in three species of grass carps.

Gene profile detection

To compare the difference of immune regulation, crucial gene patterns were detected in the midgut and liver of GC, GGC, and DRGC upon infection. In Figs. 4A and S3A, GC perfused with strain L3-3 exerted a sharp increase of cxc114, cc120, cc12, muc13a, muc5e, muc15, muc2, IgM, $tnf\alpha$, il8, il6, and mpo in the midgut, while relative expressions of cc18 and muc21 decreased sharply (p < 0.05). In Figs. 4B and S3B, relative expressions of cc12, cc18, cc120, il19, cxc118b, hepcidin, mpo, il6, il8, $tnf\alpha$, IgM, IgT/Z, cd4, and $cd8\alpha$ increased by 5.6-, 2.3-, 52.2-, 12.7-, 2.1-, 3.0-, 15.1-, 23.5-, 30.1-, 21.8-, 7.8-, 6.4-, 5.9-, and 4.7-fold in the liver, along with a sharp decline of NK-lysin, $il1\beta$, cxc114, and il34 (p < 0.05).



Fig. 1 Detection of bacterial loads in tissues. A Gene expressions of A. hydrophila hlyA in tissues of GC after gut infection with A. hydrophila. B Gene expressions of A. hydrophila hlyA in tissues of GGC after gut infection with A. hydrophila. C Gene expressions of A. hydrophila. C Gene expressions of A. hydrophila hlyA in tissues of DRGC after gut infection with A. hydrophila. The calculated data (mean ± SD) with different letters were significantly different (p < 0.05)





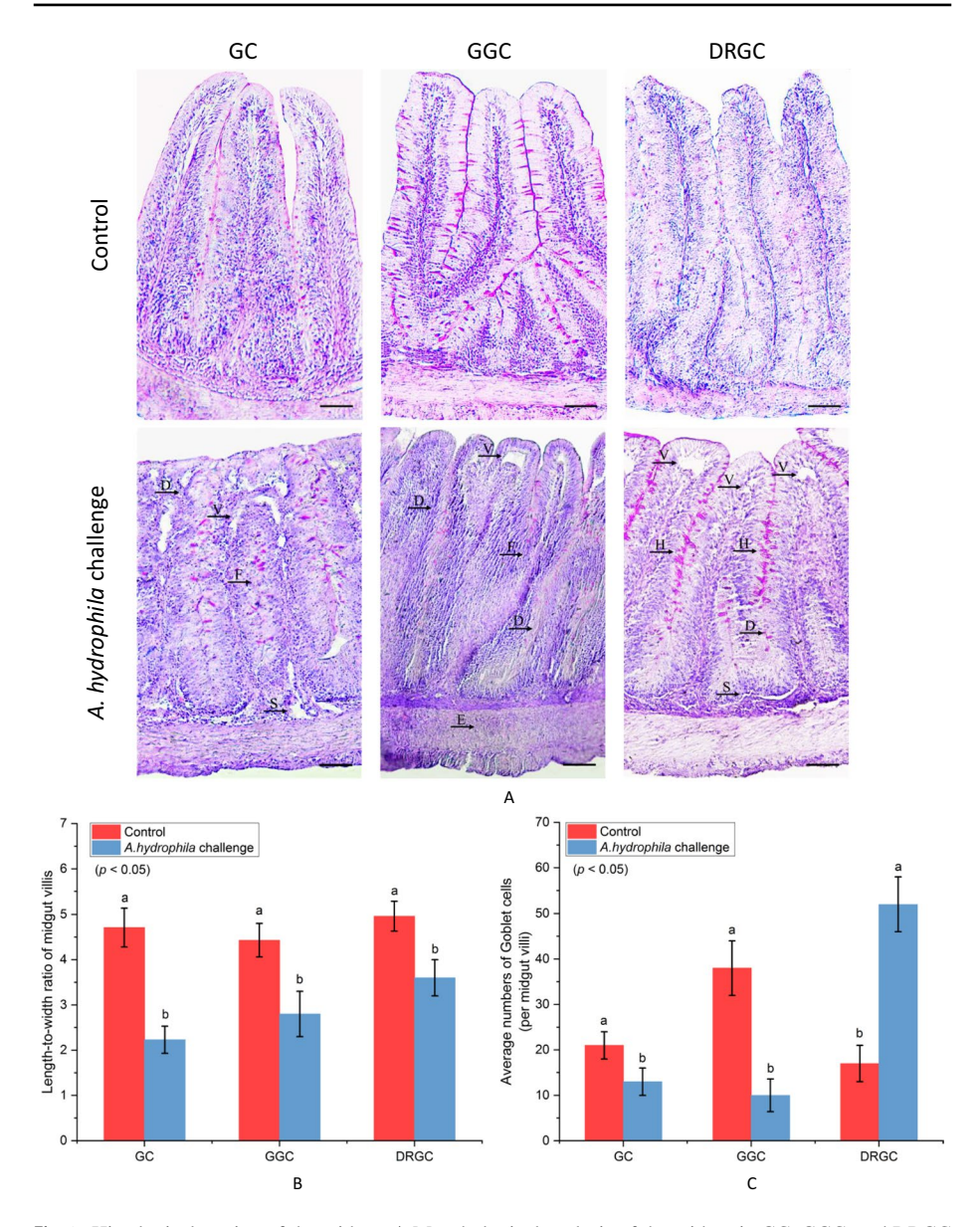


Fig. 2 Histological section of the midgut. A Morphological analysis of the midgut in GC, GGC, and DRGC anally intubated with A. hydrophila. E, edema of midgut wall; H, goblet cell hyperplasia; D, villus deformation; V, villus vacuolization; S, submucosal rupture; F, villus fusion. B Determination of length-to-width ratio in the midgut villi. C Determination of average numbers of goblet cells. Results (mean \pm SD) with different letters were significantly different (p<0.05). The experiments were performed in triplicate

In Figs. 4C and S3C, 2.1-, 1.5-, 9.5-, 6.0-, 3.1-, 1.4-, 3.0-, 7.1-, 12.5-, 16.1-, 13.8-, and 1.6-fold increase of muc2, muc15, muc5e, muc13a, ccl2, cxcl14, cxcl12a, mpo, il6, il8, $tnf\alpha$, and lgM were detected in midgut of GGC after strain L3-3 challenge, while relative expressions of ccl20, ccl8, and muc21 decreased significantly (p < 0.05). In Figs. 4D and S3D, relative expressions of il19, il34, cxcl14, cxcl12a, cxcl18b, hepcidin, mpo, il6, il8,



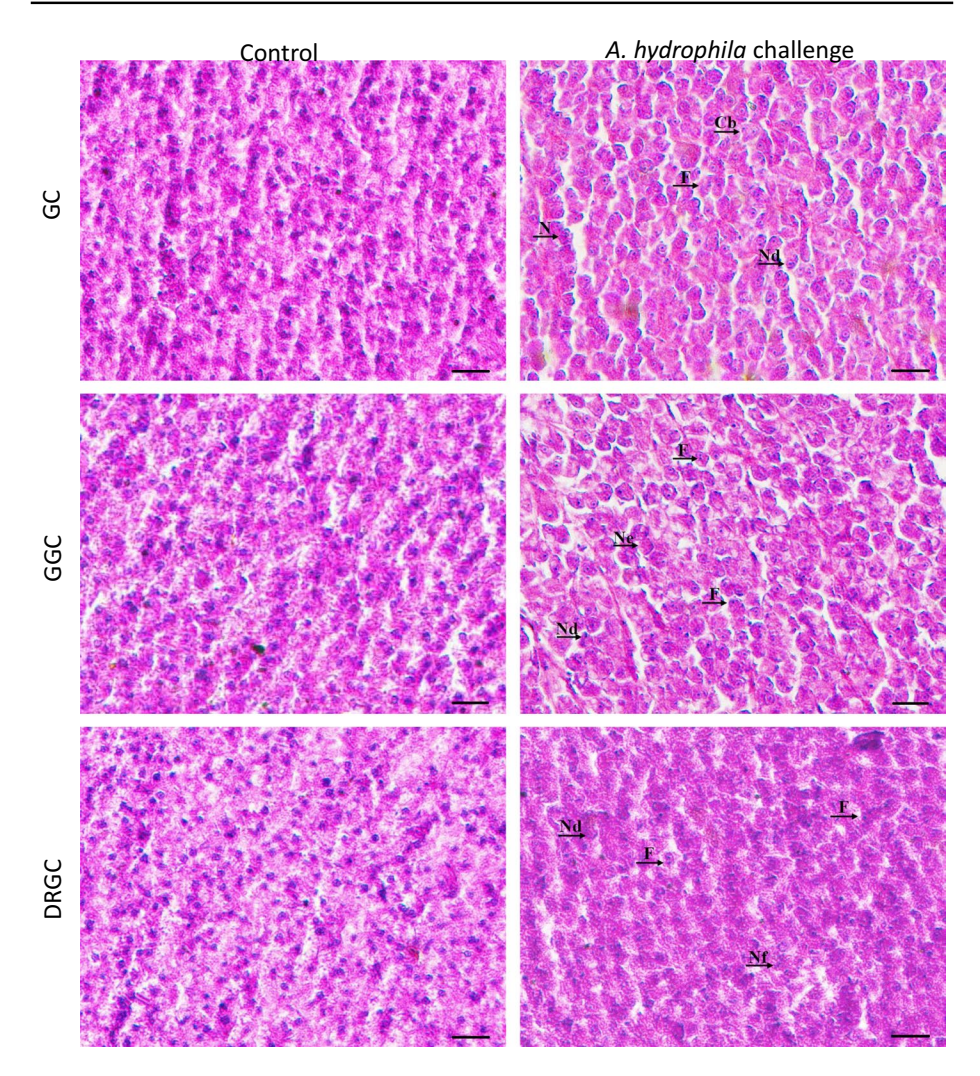


Fig. 3 Histological section of L in GC, GGC, and DRGC after gut infection with *A. hydrophila*. N, necrosis; F, fusion; Nd, nuclear displacement; Cb, cell boundary blurring; Ne, nuclear enrichment; Nf, nuclear fragmentation

 $tnf\alpha$, IgM, IgT/Z, cd4, and $cd8\alpha$ rose 1.9-, 2.6-, 10.8-, 8.4-, 14.3-, 3.1-, 13.1-, 16.5-, 23.1-, 18.8-, 4.8-, 3.2-, 2.2-, and 2.7-fold in the liver upon infection, while $il1\beta$, ccl20, and ccl8 expressions decreased dramatically (p < 0.05).

In Figs. 4E and S3E, 4.1-, 1.5-, 3.9-, 3.7-, 4.9-, 3.4-, 3.1-, 4.5-, 2.7-, 6.8-, 2.7-, 1.7-, 1.5-, and 1.7-fold increase of muc2, muc4, muc15, muc13a, ccl2, ccl8, mpo, il6, il8, $tnf\alpha$, IgM, IgT/Z, cd4, and $cd8\alpha$ were observed in midgut of DRGC after gut infection with strain L3-3, whereas relative expressions of cxcl12a, cxcl14, and muc5e decreased sharply (p < 0.05). In Figs. 4F and S3F, il19, il34, $il1\beta$, hepcidin, mpo, il6, il8, $tnf\alpha$, IgT/Z, cd4, and $cd8\alpha$ increased dramatically in the liver after strain L3-3 infection, along with a marked decline of cxcl18b, cxcl12a, cxcl14, ccl20 and ccl8 (p < 0.05).



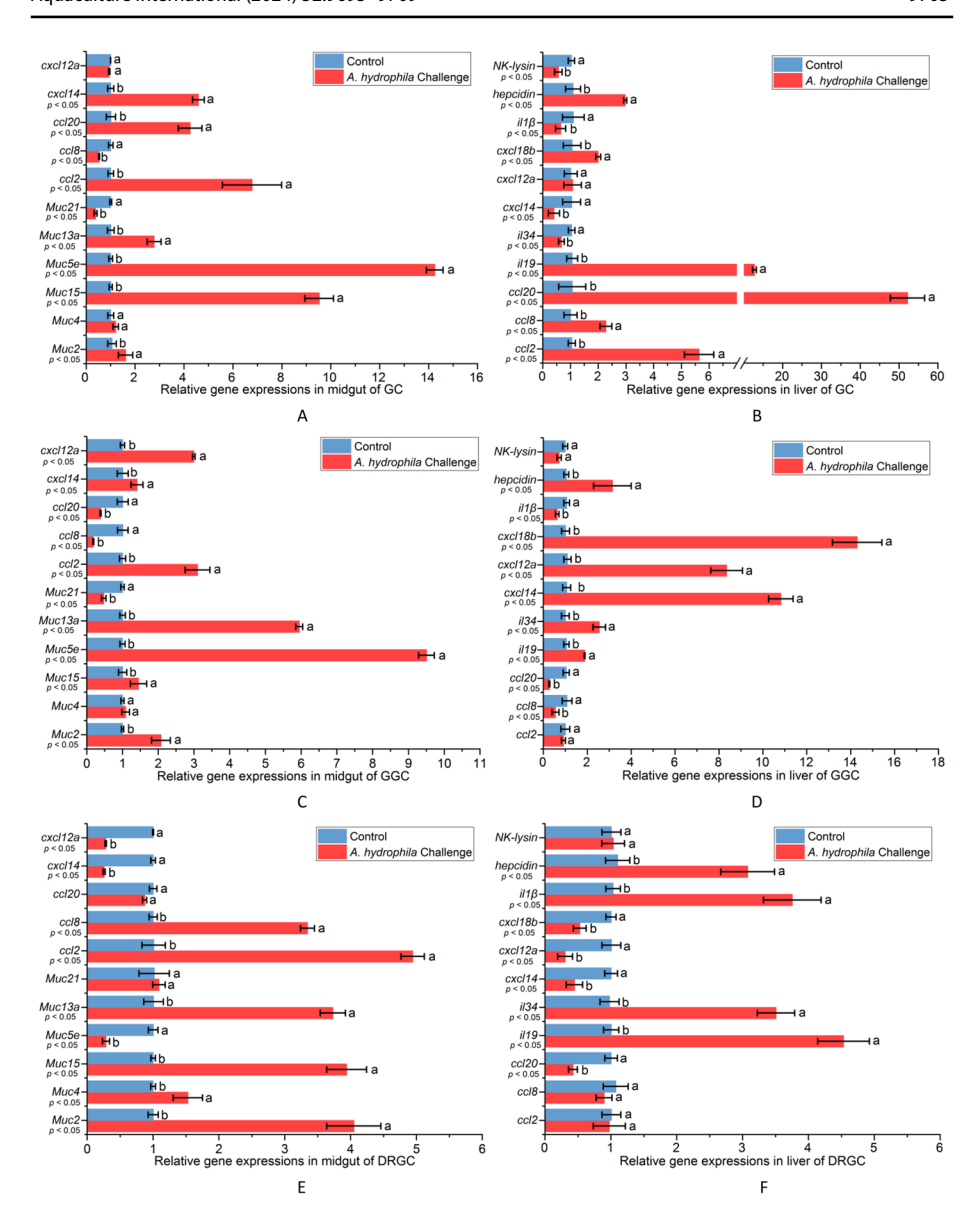


Fig. 4 Expressions of immune-relative genes in the midgut and liver after gut infection with *A. hydrophila*. **A** Gene expressions in the midgut of GC. **B** Gene expressions in the liver of GC. **C** Gene expressions in the midgut of GGC. **D** Gene expressions in the liver of GGC. **E** Gene expressions in the midgut of DRGC. **F** Gene expressions in the liver of DRGC. The calculated data (mean \pm SD) with different letters were significantly different (p < 0.05). The experiments were performed in triplicate

The changed expressions of immune-related genes in the midgut and liver were calculated by PCA. The expressions of most immune-related genes in the midgut of GC, GGC, and DRGC were predominantly located in the second and fourth quadrants, which displayed the horizontal mirror symmetry. In addition, expression level of Muc21 displayed a negative correlation with that of ccl2, muc13a, Muc15, mpo, $tnf\alpha$, and il6 (Fig. S4A).



In Fig. S4B, expression levels of cxcl14, $il1\beta$, cxcl12a, cd8, cxcl18b, and IgT/Z showed a negative correlation with il6 expression in the liver of GC, GGC, and DRGC after gut infection. Moreover, expression trends of IgM, mpo, and $tnf\alpha$ were negative-correlated with that of ccl2, ccl8, and NK-lysin. Besides, the remote distances of PCA ellipses in the midgut and liver of DRGC were much smaller than that of GC and GGC. Thus, taken together, these results suggested that most proportions of immune-related genes increased dramatically in three species of grass carps following gut infection with A. hydrophila, but amplitudes of gene expressions in DRGC were lower than that of GC and GGC.

Antioxidant property determination

To evaluate the effect of bacterial infection on redox status in three species of grass carps, antioxidant indexes were investigated in the midgut and liver. As shown in Fig. 5A, GC, GGC,
and DRGC receiving gut infection with strain L3-3 showed 1.6-, 1.7-, and 1.7-fold decrease of **CAT** activities in the midgut, respectively (p<0.05). Similarly, **SDH** activities decreased by
1.6-, 2.1-, and 1.4-fold in midgut of GC, GGC, and DRGC (p<0.05) (Fig. 5B). In contrast,
1.3-, 1.4-, and 1.3-fold increase of **GPx** activities were detected in the midgut of GC, GGC,
and DRGC, while **LDH** activities in midgut increased by 1.2-, 1.3-, and 1.6-fold (p<0.05)
(Fig. 5C, D). In addition, **GR** activities increased by 1.3- and 1.4-fold in the midgut of GC and
DRGC upon infection, whereas 1.4-fold decline of **GR** activity was observed in GGC (p<0.05)
(Fig. 5E). As shown in Fig. 5F, 1.6- and 1.3-fold increase of **MAO** activities were detected in
midgut of GC and DRGC, while **MAO** activity decreased by 2.0-fold in GGC (p<0.05).

In Fig. 6A, **CAT** activities increased by 1.4-, 1.3- and 1.5-fold in the liver of GC, GGC and DRGC after strain L3-3 challenge. In Fig. 6B, 1.6- and 1.4-fold increase of **SDH** activities were observed in the liver of GGC and DRGC upon infection, while **SDH** activity decreased by 1.7-fold in GC (p < 0.05). In Fig. 6C, 1.5-, 2.1-, and 1.7-fold increases of **GPx** activities were observed in GC, GGC, and DRGC, respectively (p < 0.05). In addition, **LDH** activities increased by 1.6-, 1.3-, and 1.4-fold in GC, GGC, and DRGC (p < 0.05) (Fig. 6D). In Fig. 6E, increased levels of **GR** activities reached the values of 1.4-, 1.4-, and 1.7-fold in GC, GGC and DRGC at 72 h post-infection, while **MAO** activities rose 1.3-, 1.3-, and 1.6-fold in the liver, respectively (p < 0.05).

The changed expressions of redox properties in the midgut and liver were calculated by PCA. The activities of most redox enzymes in the midgut of GC, GGC, and DRGC were predominantly located in the second quadrants, while GPx activities were negative-correlated with CAT activities (Fig. S4C). Moreover, activities of GPx, CAT, and MAO in the liver of three species of grass carps showed horizontal mirror symmetry with that of LDH, GR, and SDH (Fig. S4D). These results suggested that the differential redox regulation was observed in the midgut and liver of GC, GGC, and DRGC following gut infection with *A. hydrophila*.

Discussion

A. hydrophila is one of the important etiologic agents that can cause a broad range of infectious diseases in farmed animals. Stress response mechanisms can enable A. hydrophila to cope with multiple stressful conditions, which may facilitate biofilm formation to enhance its survival and evade host immune surveillance (Abreu et al. 2018). In addition, high invasiveness of A. hydrophila is largely attributed to the production of various virulent factors



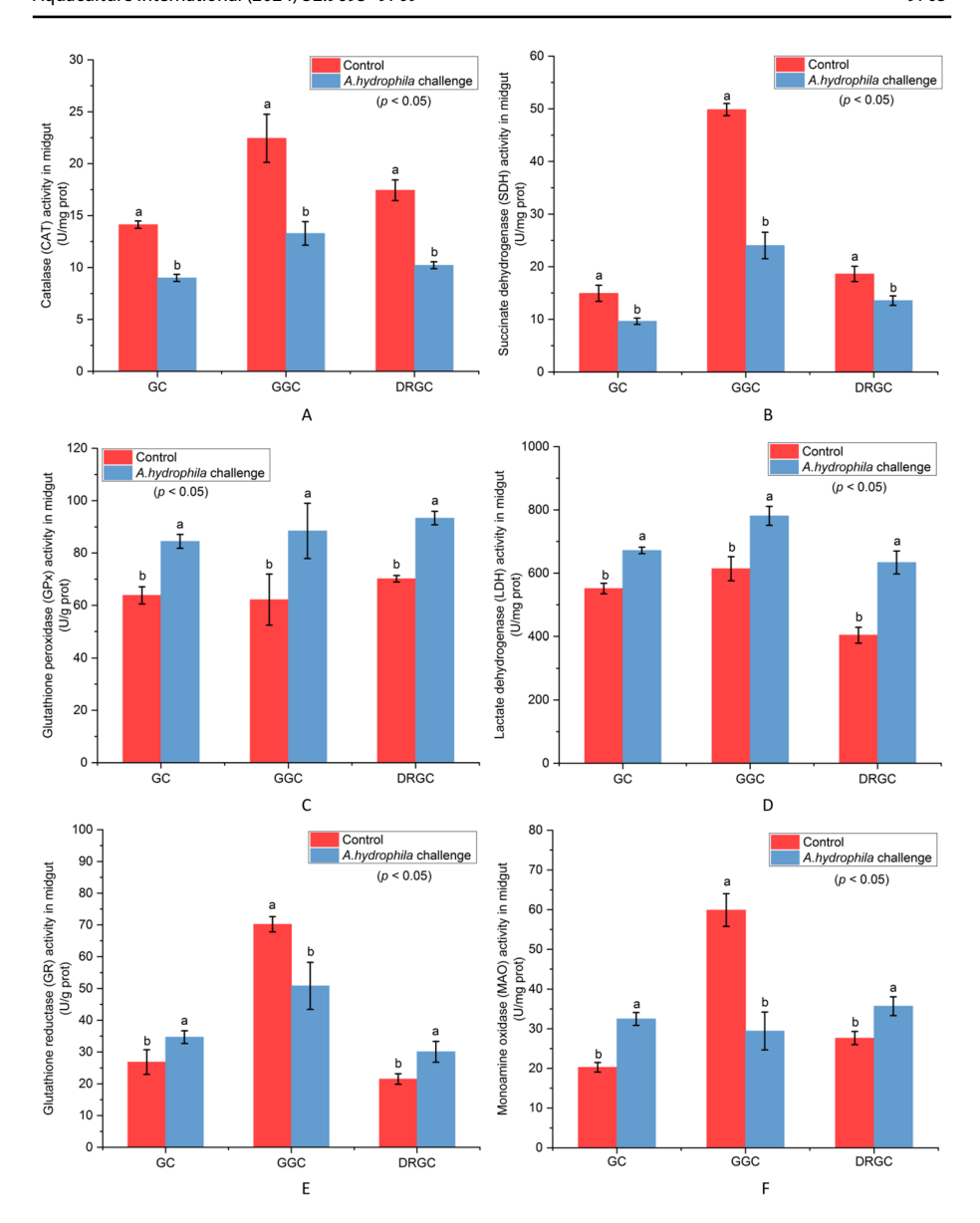


Fig. 5 Evaluation of antioxidant properties in the midgut. A–F Enzymatic activities of CAT, SDH, GPx, LDH, GR, and MAO were detected in the midgut of GC, GGC, and DRGC after gut infection with A. hydrophila. The calculated data (mean \pm SD) with different letters were significantly different (p<0.05) among the groups. The experiments were performed in triplicate

encoded by virulence genes, such as *hlyA* (Harikrishnan and Balasundaram 2005). Previous studies indicated *A. hydrophila* challenge could dramatically impair host gut barrier and exacerbate liver injury in red crucian carp (Wang et al. 2023b). In this investigation, we selected *hlyA* gene as tracking marker to identify the infectious status of three species of grass carps following gut infection with *A. hydrophila*. The elevated expressions of strain L3-3 *hlyA* were found in the liver, midgut, trunk kidney, and spleen of GC, GGC,



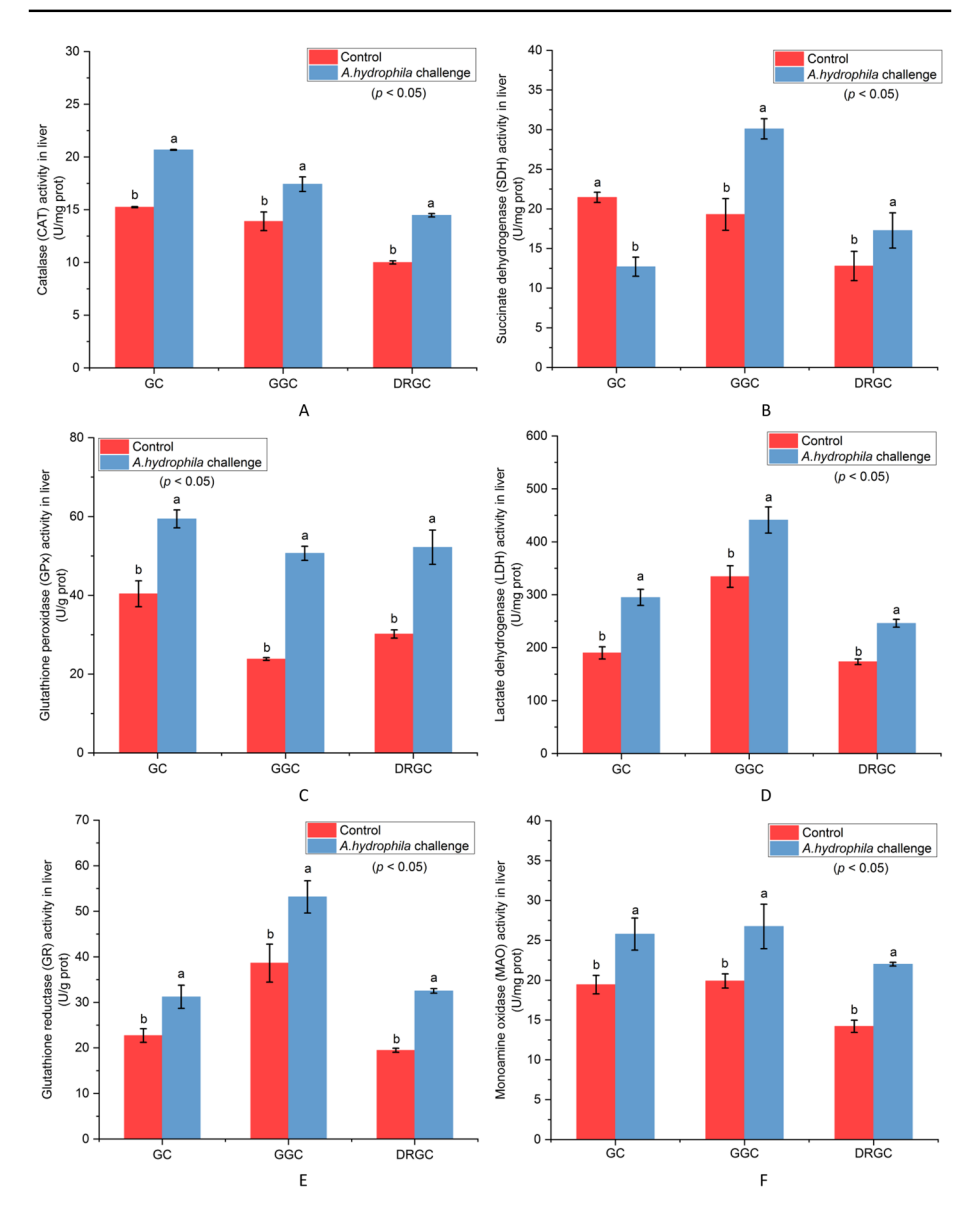


Fig. 6 Evaluation of antioxidant properties in the liver. A–F Enzymatic activities of CAT, SDH, GPx, LDH, GR, and MAO were detected in the liver of GC, GGC, and DRGC after gut infection with A. hydrophila. The calculated data (mean \pm SD) with different letters were significantly different (p<0.05) among the groups. The experiments were performed in triplicate

and DRGC after bacterial challenge. Besides, high expressions of *A. hydrophila hlyA* gene were observed in the midgut and spleen of GC, while the trunk kidney and spleen of GGC showed high levels of *A. hydrophila hlyA* gene. In contrast, high level of *A. hydrophila hlyA* gene was only detected in the spleen of DRGC. These results suggested that *A. hydrophila* L3-3 may breach gut barrier and lead to systemic infection in three species of grass carps, which may display the different tolerance against *A. hydrophila* invasion.



Afterwards, histological section assays revealed that pathological injuries in the midgut and liver of GC and GGC appeared to be more severe than that of DRGC. In addition, goblet cell numbers decreased dramatically in the midgut villi of GC and GGC after gut infection with strain L3-3, while goblet cell hyperplasia occurred in the midgut villi of DRGC. As is well known, gut epithelial cells serving as critical sensors of foreign stimuli not only effectively orchestrate mucosal immunity by attraction of active immune cells (Soderholm and Pedicord 2019), but also establish the crucial barrier against invading pathogens (Schneeberger and Lynch 2004). Goblet cells can secret mucins and immune macromolecules to mediate mucosal immune response to pathogenic infection (Kim and Ho 2010). In the meantime, the liver is the pivotal immune-related organ involved in regulation of microbial elimination processes via multiple signals, which can receive substances from the gut tract and then promote the production of antimicrobial molecules (Bayne and Gerwick 2001; Gao et al. 2008). Recently, some reports indicated that cytokine and chemokine may regulate the production of antimicrobial peptides (AMPs) (Kolls et al. 2008) or directly exhibit antimicrobial activities (Wolf and Moser 2012). **NK-lysin** and **hepcidin** are the important fish AMPs that can be involved in the front line of bacterial killing mechanism (Luo et al. 2021; Wang et al. 2010). Generally speaking, cytokine production and secretion participate in host immune regulation and enhance disease tolerance against invasive microbes (Wu et al. 2016), which can regulate the immune cell activation and contribute to inflammatory processes at inflamed organs upon infection (Gouwy et al. 2005), but the defect in built-in checkpoints and anti-inflammatory signals may undoubtedly predispose to the outbreak of chronic inflammatory diseases (Lawrence and Gilroy 2007). In this investigation, most proportion of mucins, cytokines, and AMPs elevated markedly in the midgut and liver of three species of grass carps after bacterial gut infection, along with differential redox response, while fluctuations of gene expressions in DRGC were lower than that of GC and GGC. Thus, taken together, we predicted that DRGC may exhibit a higher tolerance against A. hydrophila-induced tissue inflammation.

Inflammatory process is tightly linked to oxidative stress, which may further contribute to perpetuation of inflammatory diseases (Lugrin et al. 2014). Evidences are emerging that bacterial infection may also trigger severe oxidative stress and alter antioxidant enzymatic activities in teleost fish (Peixoto et al. 2018). MAO and SDH are two important enzymatic biomarkers of mitochondria, whose abnormal expressions may reflect the dysfunction of oxidative phosphorylation in mitochondria (Seregi et al. 1983). Mitochondrial dysfunction may promote elevated levels of reactive oxygen species (ROS), whose chronic upregulation may exhibit the detrimental effort on function of intracellular macromolecules (Bolisetty and Jaimes 2013). In addition, increased LDH activities were highly associated with worse outcomes in fish under infection status (Yarahmadi et al. 2016). Recent findings indicate that antioxidant enzymes are able to partially inhibit stress-induced ROS production through the regulation of redox-dependent defense against in vitro stimuli (Hoseinifar et al. 2020). Among known antioxidant enzymes, CAT, GPx, and GR are playing pivotal role in fish immunity, which can immediately attenuate stress-induced oxidative level and ROS cytotoxicity (Li et al. 2016). Current study revealed that most detected redox enzymes increased dramatically in the midgut and liver of GC, GGC, and DRGC after strain L3-3 challenge and suggested that gut infection stimulated a dramatic fluctuation of antioxidant capability in the midgut and liver of GC, GGC, and DRGC.

In summary, increased bacterial loads in tissues were determined in GC, GGC, and DRGC after gut infection with *A. hydrophila*. After that, more severe pathological injuries and higher expressions of inflammatory cytokines were observed in the midgut and liver of GC and GGC by comparing with that of DRGC, along with increased levels of antioxidant activities. Thus, these results may provide a novel understanding of immune and redox regulation of hybrid grass carp upon infection.



Supplementary Information The online version contains supplementary material available at https://doi.org/10.1007/s10499-024-01634-w.

Author contributions Wei-Sheng Luo and Zi-Han Xu performed methodology, data curation and formal analysis; Qin-Yang He, Jie Peng, Fei Wang and Jian Li performed validation; Sheng-Wei Luo performed conceptualization, supervision, project management and article writing.

Data availability No datasets were generated or analysed during the current study.

Declarations

Competing interests The authors declare no competing interests.

References

- Abreu RE, Magalhães TC, Souza RC, Oliveira ST, Ibelli AM, Demarqui FN et al (2018) Environmental factors on virulence of Aeromonas hydrophila. Aquacult Int 26:495–507
- Bayne CJ, Gerwick L (2001) The acute phase response and innate immunity of fish. Dev Comp Immunol 25:725–743
- Bolisetty S, Jaimes EA (2013) Mitochondria and reactive oxygen species: physiology and pathophysiology. Int J Mol Sci 14:6306–6344
- Boltaña S, Roher N, Goetz FW, MacKenzie SA (2011) PAMPs, PRRs and the genomics of gram negative bacterial recognition in fish. Dev Comp Immunol 35:1195–1203
- Bullini L (1985) Speciation by hybridization in animals. Italian Journal of Zoology 52:121-137
- Gao B, Jeong WI, Tian Z (2008) Liver: an organ with predominant innate immunity. Hepatology 47:729–736
- Giuffrè M, Campigotto M, Campisciano G, Comar M, Crocè LS (2020) A story of liver and gut microbes: How does the intestinal flora affect liver disease? A review of the literature. Am J Physiol-Gastroint Liver Physiol Gastrointest 318:G889-G906
- Gouwy M, Struyf S, Proost P, Van Damme J (2005) Synergy in cytokine and chemokine networks amplifies the inflammatory response. Cytokine Growth Factor Rev 16:561–580
- $Harikrishnan\ R,\ Balasundaram\ C\ (2005)\ Modern\ trends\ in\ Aeromonas\ hydrophila\ disease\ management\ with$ $fish.\ Rev\ Fish\ Sci\ 13:281-320$
- Hoseinifar SH, Yousefi S, Van Doan H, Ashouri G, Gioacchini G, Maradonna F et al (2020) Oxidative stress and antioxidant defense in fish: the implications of probiotic, prebiotic, and synbiotics. Reviews in Fisheries Science & Aquaculture 29:198–217
- Howard SP, Garland WJ, Green MJ, Buckley JT (1987) Nucleotide sequence of the gene for the hole-forming toxin aerolysin of Aeromonas hydrophila. J Bacteriol 169:2869–2871
- Kania PW, Buchmann K (2022) Complement activation in fish with emphasis on MBL/MASP. In Principles of fish immunology: from cells and molecules to host protection. Cham: Springer International Publishing, pp 279–300
- Kim YS, Ho SB (2010) Intestinal goblet cells and mucins in health and disease: recent insights and progress. Curr Gastroenterol Rep 12:319–330
- Kolls JK, McCray PB Jr, Chan YR (2008) Cytokine-mediated regulation of antimicrobial proteins. Nat Rev Immunol 8:829–835
- Lawrence T, Gilroy DW (2007) Chronic inflammation: a failure of resolution? Int J Exp Pathol 88:85-94
- Li M, Gong S, Li Q, Yuan L, Meng F, Wang R (2016) Ammonia toxicity induces glutamine accumulation, oxidative stress and immunosuppression in juvenile yellow catfish Pelteobagrus fulvidraco. Comp Biochem Physiol c: Toxicol Pharmacol 183:1–6
- Li S-Y, Xiong N-X, Li K-X, Huang J-F, Ou J, Wang F et al (2024) Cloning, expression and functional characterization of recombinant tumor necrosis factor α1 (TNFα1) from white crucian carp in gut immune regulation. Int J Biol Macromol 254:127770
- Lugrin J, Rosenblatt-Velin N, Parapanov R, Liaudet L (2014) The role of oxidative stress during inflammatory processes. Biol Chem 395:203–230
- Luo S-W, Xiong N-X, Luo Z-Y, Fan L-F, Luo K-K, Mao Z-W et al (2021) A novel NK-lysin in hybrid crucian carp can exhibit cytotoxic activity in fish cells and confer protection against Aeromonas hydrophila infection in comparison with Carassius cuvieri and Carassius auratus red var. Fish Shellfish Immunol 116:1–11



- Ma X, Wang Y, Yin H, Hua L, Zhang X, Xiao J et al (2021) Down-regulated long non-coding RNA RMST ameliorates dopaminergic neuron damage in Parkinson's disease rats via regulation of TLR/NF-κB signaling pathway. Brain Res Bull 174:22–30
- Magnadottir B (2010) Immunological control of fish diseases. Mar Biotechnol 12:361-379
- Peixoto M, Domingues A, Batista S, Gonçalves J, Gomes A, Cunha S et al (2018) Physiopathological responses of sole (Solea senegalensis) subjected to bacterial infection and handling stress after probiotic treatment with autochthonous bacteria. Fish Shellfish Immunol 83:348–358
- Pickard JM, Zeng MY, Caruso R, Núñez G (2017) Gut microbiota: Role in pathogen colonization, immune responses, and inflammatory disease. Immunol Rev 279:70–89
- Reid S, McDonald D, Wood C (1997) Interactive effects of temperature and pollutant stress. In: Society of experimental biology seminar series, pp 325–349
- Schneeberger EE, Lynch RD (2004) The tight junction: a multifunctional complex. Am J Physiol Cell Physiol 286:C1213–C1228
- Secombes C, Wang T, Hong S, Peddie S, Crampe M, Laing K et al (2001) Cytokines and innate immunity of fish. Dev Comp Immunol 25:713–723
- Seregi A, Serfózó P, Mergl Z (1983) Evidence for the localization of hydrogen peroxide-stimulated cyclooxygenase activity in rat brain mitochondria: a possible coupling with monoamine oxidase. J Neurochem 40:407–413
- Soderholm AT, Pedicord VA (2019) Intestinal epithelial cells: at the interface of the microbiota and mucosal immunity. Immunology 158:267–280
- Trivedi PJ, Adams DH (2016) Gut-liver immunity. J Hepatol 64:1187-1189
- Wang Y-D, Kung C-W, Chen J-Y (2010) Antiviral activity by fish antimicrobial peptides of epinecidin-1 and hepcidin 1–5 against nervous necrosis virus in medaka. Peptides 31:1026–1033
- Wang Y, Tan H, Li M, Geng C, Wang S, Zhao R et al (2022) The comparative studies on growth rate and disease resistance between improved grass carp and common grass carp. Aquaculture 560:738476
- Wang C, Luo X, Zhang Y, Zhou Y, Xiao Q, Huang X et al (2023a) Triploidization modulates intestinal microbiota and promotes growth in Carassius auratus. Aquaculture 571:739480
- Wang F, Qin Z-L, Luo W-S, Xiong N-X, Luo S-W (2023b) Aeromonas hydrophila can modulate synchronization of immune response in gut-liver axis of red crucian carp via the breach of gut barrier. Aquac Int 2023:1–15
- Wang F, Qin ZL, Luo WS, Xiong NX, Huang MZ, Ou J et al (2023c) Alteration of synergistic immune response in gut–liver axis of white crucian carp (Carassius cuvieri) after gut infection with Aeromonas hydrophila. J Fish Dis 00:1–11
- Wolf M, Moser B (2012) Antimicrobial activities of chemokines: not just a side-effect? Front Immunol 3:213
- Wu N, Song Y-L, Wang B, Zhang X-Y, Zhang X-J, Wang Y-L et al (2016) Fish gut-liver immunity during homeostasis or inflammation revealed by integrative transcriptome and proteome studies. Sci Rep 6:1–17
- Xie C, Li J, Li D, Shen Y, Gao Y, Zhang Z (2018) Grass carp: the fish that feeds half of China. Aquaculture in China: Success stories and modern trends, pp 93–115. https://doi.org/10.1002/9781119120759.ch2_1
- Xiong N-X, Luo S-W, Fan L-F, Mao Z-W, Luo K-K, Liu S-J et al (2021) Comparative analysis of erythrocyte hemolysis, plasma parameters and metabolic features in red crucian carp (Carassius auratus red var) and triploid hybrid fish following Aeromonas hydrophila challenge. Fish Shellfish Immunol 118:369–384
- Xiong NX, Kuang XY, Fang ZX, Ou J, Li SY, Zhao JH et al (2022) Transcriptome analysis and co-expression network reveal the mechanism linking mitochondrial function to immune regulation in red crucian carp (Carassius auratus red var) after Aeromonas hydrophila challenge. J Fish Dis 45:1491–1509
- Xiong N-X, Wang F, Luo W-S, Ou J, Qin Z-L, Huang M-Z, Luo SW (2023) Tumor necrosis factor α2 (TNFα2) facilitates gut barrier breach by Aeromonas hydrophila and exacerbates liver injury in hybrid fish. Aquaculture 577:739995
- Yarahmadi P, Farsani HG, Khazaei A, Khodadadi M, Rashidiyan G, Jalali MA (2016) Protective effects of the prebiotic on the immunological indicators of rainbow trout (Oncorhynchus mykiss) infected with Aeromonas hydrophila. Fish Shellfish Immunol 54:589–597
- Yuan X, Lv Z, Zhang Z, Han Y, Liu Z, Zhang H (2023) A review of antibiotics, antibiotic resistant bacteria, and resistance genes in aquaculture: Occurrence, contamination, and transmission. Toxics 11:420 Zeuzem S (2000) Gut-liver axis. Int J Colorectal Dis 15:59–82

Publisher's Note Springer Nature remains neutral with regard to jurisdictional claims in published maps and institutional affiliations.

Springer Nature or its licensor (e.g. a society or other partner) holds exclusive rights to this article under a publishing agreement with the author(s) or other rightsholder(s); author self-archiving of the accepted manuscript version of this article is solely governed by the terms of such publishing agreement and applicable law.

